2024 년 2 월
석사학위 논문

# Regulation of *Dictyostelium* Development by RapC and Functional Changes of Ras Proteins by the C-terminus of RapC

조 선 대 학 교 대 학 원

글로벌바이오융합학과

한 나 라

# Regulation of *Dictyostelium* Development by RapC and Functional Changes of Ras Proteins by the C-terminus of RapC

**RapC** 에 의한 딕티오스텔리움 발달과정 조절 및
**RapC** 말단 부위에 의한 **Ras** 단백질의 기능 변화 연구

**2024** 년 **2** 월 **23** 일

조 선 대 학 교 대 학 원

글로벌바이오융합학과

한 나 라

# Regulation of *Dictyostelium* Development by RapC and Functional Changes of Ras Proteins by the C-terminus of RapC

지도교수 전 택 중

이 논문을 이학 석사학위신청 논문으로 제출함

**2023 년 10 월**

조 선 대 학 교 대 학 원

글로벌바이오융합학과

한 나 라

# 한나라의 석사학위논문을 인준함

위원장 이 준 식 (인)

위 원 전 택 중 (인)

위 원 조 광 원 (인)

**2023 년 12 월**

## 조 선 대 학 교 대 학 원

# CONTENTS

# ABBREVIATIONS

| | |
|---|---|
| ACA | Adenyl cyclase A |
| Als | Activation loops |
| AMPK | AMP-activated protein kinase |
| cAMP | Cyclic adenosine monophosphate |
| GAPs | GTPase activating proteins |
| GDP | Guanine diphosphate |
| GEFs | Guanine nucleotide exchange factors |
| GFP | Green fluorescent protein |
| GTP | Guanine triphosphate |
| HMs | Hydrophobic motifs |
| mTORC2 | Mechanistic target of rapamycin complex 2 |
| PBS | Phosphate-buffered saline |
| PCR | Polymerase chain reaction |
| PDK | Phosphoinositide dependent kinase |
| PI3K | Phosphatidylinositol 3-kinase |
| SD | Standard deviation |
| SEM | Standard error of measurement |

# ABSTRACT

## Regulation of *Dictyostelium* Development by RapC and Functional Changes of Ras Proteins by the C-terminus of RapC

Nara Han

Advisor: Prof. Taeck Joong Jeon, Ph.D.

Department of Integrative Biological Sciences,

Graduate School of Chosun University

Ras proteins are small GTPases that act as molecular switches in various cellular processes. There are three Rap proteins in *Dictyostelium*: RapA, RapB, and RapC. Rap proteins are key regulators in cell adhesion and cytoskeleton rearrangement. RapC has a unique function in regulating multicellular development. When *Dictyostelium* cells are starved, they secrete cAMP, a chemoattractant, and form multicellular mound through aggregation. The aggregates undergo differentiation processes and finally form spores. During this process, wild-type cells form single tip that forms one fruiting body from one multicellular mound. Whereas cells lacking RapC form multiple tips from one multicellular mound. While I investigate the mechanism by which RapC regulates the developmental process of *Dictyostelium*, I found that multi-tips were formed when wild-type cells were treated with caffeine. Caffeine is an antagonist of adenosine receptor and affects the cAMP signaling pathway in *Dictyostelium*. Therefore, I investigated the mechanism for the regulation of developmental process by RapC based on the caffeine-mediated cAMP signaling pathway. First, I examined the development of wild-type cells in the presence of caffeine. As expected, wild-type KAx3 cells formed some multi-tips similar to *rapC* null cells in the presence of 2 mM caffeine. No developmental progress was observed above 3 mM caffeine. Since PI3K and mTORC2 are at the center of the caffeine-mediated cAMP signaling pathway,

next. I checked the effects of Torin2 and LY294002 on multicellular development, which are inhibitors of mTORC2 and PI3K, respectively. In wild-type cells, some multi-tips were formed at 1 μM Torin2, whereas a single tip was formed at 30 μM LY294002. These results suggest that the TOR signaling pathway is involved in multi-tip formation process. The TOR complex consists of TOR1 and TOR2. To determine which TOR complex affects the developmental process, I examined the multicellular development of the cells in the presence of 50 nM rapamycin, a mTORC1 inhibitor. Wild-type cells formed some multi-tips at 50 nM rapamycin, indicating that TOR complex1 plays an important role in the developmental process, especially at the tip forming stage of the development. These results suggest that RapC is involved in *Dictyostelium* development through regulation TOR complex pathway.

In *Dictyostelium*, RapA and RapC have been reported to have opposite functions in cell adhesion and cell migration. RapC has a longer amino acid tail than RapA at the C-terminus. When the C-terminus of RapC was fused to the end of RapA, the function of RapA was reversed. The recombinant RapA-CT had the same function as RapC in cell adhesion and cell migration. In the presence study, to determine whether the C-terminus of RapC can reverse the functions of other Ras proteins, I fused the C-terminus of RapC to the end of RasG, which has the most similar function to RapA among Ras proteins. RasG fused with C-terminus of RapC (RasG-CT) was expressed in *rapC* null cells and *rasG* null cells, and the phenotypes were compared those of wild-type cells. *rapC* null cells expressing RasG-CT showed spread morphology and increased adhesion than wild-type cells. During development, *rapC* null cells expressing RasG-CT formed multi-tips. The migration speed in chemotaxis was significantly reduced compared to wild-type cells. These results were identical to the phenotypes of *rapC* null cells. This suggests that the C-terminus of RapC is unable to reverse the functions of RasG. On the other hand, *rasG* null cells showed increased cell size and decreased adhesion compared to wild-type cells. During development, *rasG* null cells formed small spores than wild-types cells. *rasG* null cells expressing RasG-CT were similar to wild-type cells in cell size, adhesion and developmental

process. In random cell migration, *rasG* null cells showed higher migration speed than wild-type cells, but *rasG* null cells expressing RasG-CT displayed the migration speed similar to wild-type cells. In electrotaxis, *rasG* null cells showed increased migration speed and decreased directionality than wild-type cells. These phenotypes of *rasG* null cells were restored by expression of RasG-CT. These results suggest that the C-terminus of RapC is able to reverse the functions of the Rap proteins, but not other Ras proteins.

# 국문초록

## RapC 에 의한 딕티오스텔리움 발달과정 조절 및 RapC 말단 부위에 의한 Ras 단백질의 기능 변화 연구

한 나 라

지도교수: 전 택 중

글로벌바이오융합학과

조선대학교 대학원

Ras 단백질들은 다양한 세포 과정에서 분자적 스위치 역할을 하는 작은 GTPases 이다. 딕티오스텔리움 내에는 RapA, RapB, 그리고 RapC 의 3 가지 Rap 단백질이 존재한다. Rap 단백질들은 세포 부착과 세포골격 재배열의 주요 조절자이다. 이전의 연구에서, RapC 는 세포의 발달과정을 조절하는데 독특한 기능을 하는 것으로 알려졌다. 딕티오스텔리움 세포는 기아 상태가 되면 화학유인물질인 cAMP 를 분비하고 응집을 통해 다세포 마운드를 형성한다. 응집체들은 분화과정을 거쳐 최종적으로 포자를 형성한다. 이 과정동안, 야생형 세포는 1 개의 다세포 마운드에서 1 개의 자실체를 형성하는 단일 팁을 형성한다. 반면, RapC 가 결여된 세포는 1 개의 다세포 마운드에서 여러 개의 팁을 형성한다. RapC 가 딕티오스텔리움 발달과정을 조절하는 메커니즘을 조사하던 중, 야생형 세포에 카페인을 처리하면 다중 팁이 형성된다는 사실을 알게 되었다. 카페인은 아데노신의 수용체의 길항제이며, 딕티오스텔리움 내 cAMP 신호전달 경로에 영향을 미친다. 따라서 카페인 매개 cAMP 신호전달 경로를 기반으로 하여 RapC 에 의한 발달과정

조절 메커니즘에 대한 연구하였다. 가장 먼저, 카페인의 존재 하에 야생형 세포의 발달과정을 조사하였다. 예상대로, 야생형 KAx3 세포는 2 mM 카페인의 존재 하에서 *rapC* null 세포와 유사한 다중 팁을 일부 형성하였다. 3 mM 이상의 카페인 농도에서는 발달의 진행이 관찰되지 않았다. 카페인 매개 cAMP 신호전달 경로의 중심에는 PI3K 와 mTORC2 가 존재하기 때문에, 다음으로 각각 mTORC2 및 PI3K 억제제인 Torin2 와 LY294002 가 다세포 발달과정에 미치는 영향을 확인하였다. 야생형 세포는 1 μM Torin2 에서는 일부 다중 팁을 형성한 반면, 30 μM LY294002 에서는 단일 팁을 형성하였다. 이러한 결과들은 TOR 신호 전달 경로가 다중 팁 형성 과정에 관여한다는 것을 시사한다. TOR 복합체는 TOR1 과 TOR2 로 구성된다. 어떤 TOR 복합체가 발달과정에 영향을 미치는지 확인하기 위해, mTORC1 의 억제제인 50 nM rapamycin 의 존재 하에서 다세포 발달과정을 조사하였다. 야생형 세포는 50 nM 라파마이신에서 일부 다중 팁을 형성했는데, 이는 TORC1 복합체가 발달과정, 특히 발달과정의 팁 형성 단계에서 중요한 역할을 한다는 것을 나타낸다. 이러한 결과는 RapC 가 TOR 복합체 경로 조절을 통해 *Dictyostelium* 발달과정에 관여하고 있음을 시사한다.

딕티오스텔리움에서 RapA 와 RapC 는 세포 부착과 세포 이동에서 서로 반대 기능을 하는 것으로 보고되었다. RapC 는 C-말단에 RapA 보다 긴 아미노산 꼬리를 가지고 있다. RapC 의 C-말단이 RapA 의 말단에 융합되면 RapA 의 기능이 역전되었다. 재조합 RapA-CT 는 세포 부착과 세포 이동에서 RapC 와 동일한 기능을 가졌다. 본 연구에서, RapC 의 C-말단이 Ras 단백질의 기능을 역전되는지 확인하기 위해, Ras 단백질 중 RapA 와 가장 유사한 기능을 하는 RasG 말단에 RapC 의 C-말단을 융합시켰다. 이후, RapC 의 C-말단과 융합된 RasG (RasG-CT)는 *rapC* null 세포와 *rasG* null 세포에 발현되었고, 표현형은 야생형 세포의 표현형과 비교되었다. RasG-CT 를 발현하는 *rapC* null 세포는 야생형 세포보다 확산된 세포 형태를 보였고 부착력이 증가하였다. 발달과정에서 RasG-CT 를 발현하는

*rapC* null 세포는 다중 팁을 형성하였다. 주화성 이동에서는 야생형 세포에 비해 이동속도가 크게 감소하였다. 이러한 결과들은 *rapC* null 세포의 표현형과 동일했다. 이는 RapC 의 C-말단이 RasG 의 기능을 역전시킬 수 없음을 시사한다. 한편, *rasG* null 세포는 야생형 세포에 비해 세포 크기와 접착력이 감소한 것으로 나타났다. 발달 과정에서 *rasG* null 세포는 야생형보다 작은 크기의 포자를 형성하였다. RasG-CT 를 발현하는 *rasG* null 세포는 세포 형체, 부착력 및 발달과정에서 야생형 세포의 표현형과 유사했다. 무작위 세포 이동에서 *rasG* null 세포는 야생형 세포보다 높은 이동 속도를 보였지만 RasG-CT 를 발현하는 *rasG* null 세포는 야생형 세포와 비슷한 이동 속도를 보였다. 주전성 이동에서 *rasG* null 세포는 야생형 세포보다 이동 속도가 증가하고 방향성이 감소한 것으로 나타났다. *rasG* null 세포의 이러한 표현형은 RasG-CT 의 발현에 의해 복원되었다. 이러한 결과들은 RapC 의 C-말단이 Rap 단백질의 기능을 역전시킬 수 있지만 다른 Ras 단백질은 역전시킬 수 없음을 시사한다.

# PART I. Regulation of *Dictyostelium* Development by RapC

## I. Introduction

*Dictyostelium discoideum* is a unicellular free-living soil amoeba. It has a unique cycle of growth and multicellular development depending on the nutritional environment. In nutrient-rich environment, *Dictyostelium* cells live as single cells. Whereas, when starvation begins, cells secrete cAMP, a chemoattractant, and form multicellular aggregates through chemotactic migration. These multicellular aggregates then form slugs composed of anterior prestalk cells and posterior prespore cells. Slugs go through a differentiation process to form a fruiting body of dead stalk and spore mass. In this process, typical cells form one tip from a multicellular aggregate (Chisholm and Firtel, 2004; Williams, 2006; Loomis, 2015).

*Dictyostelium* contains Ras subfamily proteins, which acts as a switch in several cellular processes including cell migration, differentiation, and proliferation. Among the Ras subfamily proteins, there are three Rap proteins, RapA, RapB, and RapC. Rap proteins are known to play a key role in cytoskeleton rearrangement and cell adhesion (Kortholt and van Haastert, 2008; Raaijmakers and Bos, 2009). RapC has a unique function in regulating multicellular development of *Dictyostelium*. Cells lacking RapC formed multi-tips from a multicellular aggregate during development (Park et al., 2018). It suggests RapC is involved in regulating development of *Dictyoetslium*, but its regulatory mechanism has not yet been characterized.

Caffeine is well known as a factor causing multi-tips in *Dictyostelium* development. Caffeine is commonly used to inhibit adenyl cyclase and the synthesis of cAMP in *Dictyostelium*. Caffeine is known to be optimally effective at a concentration of 3 mM in development (Brenner and Thoms, 1984; Jaiswal et al., 2012). In addition, caffeine also has been known to inhibits PI3K and mTORC2. In *Dictyostelium*, PI3K and mTORC2 are centered in cAMP signaling

pathway, and they are required for ACA activity and cAMP production in response to extracellular cAMP stimulation (Devreotes et al., 2017; Tariqul Islam et al., 2019).

Here, I investigated the mechanism for the regulation of developmental process by RapC based on the caffeine-mediated cAMP signaling pathway. The results suggest that TOR signaling pathway is involved in multi-tip formation process, and TORC1 plays an important role in the tip forming stage of development.

# II. Materials and Methods

## II-1. Strains and cell culture

*Dictyostelium* wild-type KAx3 cells were obtained from the Stock Center (DictyBase). All the cells were grown in HL5 medium or in association with Klebsilla aerogenes at 22 ℃. Knock-out strains and transformants were maintained in 10 μg/mL blasticidin and 10 μg/mL G418. The full coding sequences of the *rapC* cDNA were generated by RT-PCR and were cloned into the *Eco*RI -*Xho*I site of the expression vector pEXP-4(+) containing a GFP fragment at the N-terminus (Park *et al.*, 2018; Jeon et al., 2007). For immunoblotting, cells were developed by pulsing with 40 nM cAMP every 5 min for 6 h in 12 mM Na/K phosphate buffer (pH 6.1).

## II-2. Reagents

Caffeine was purchased from Alfa Aesar (USA). Stock solution of caffeine (100 mM) was prepared in D.W and then added to a final concentration of 2 mM. LY294002 and dimethyl sulfoxide (DMSO) were purchased from Signa-Aldrich (St. Louis, MO, USA). Strock solution of LY294002 (50 mM) was prepared in DMSO and then added to a final concentration of 30 μM. Torin2 was purchased from ApexBio (Houston, TX, USA). Stock solution of Torin2 (10 mM) was prepared in DMSO. Torin2 was diluted to 100 μM in 12 mM Na/K Phosphate buffer before use in the experiment and added to a final concentration of 30 μM. Rapamycin was purchased from MCE (USA). Stock solution of Rapamycin (10 mM) was prepared in DMSO. Rapamycin was diluted to 100 μM in 12 mM Na/K Phosphate buffer before use in the experiment and added to a final concentration of 50 nM.

## II-3. Measurement of plasma membrane PH-CRAC

Aggregation-competent cells were prepared by pulsing with 30 uM cAMP every 6 min for 6 h in 12 mM Na/K phosphate buffer (pH 6.1) at a density of 5 x $10^6$ cells/ml with a constant shaking (150 rpm). Before to assays, 1.9 ml of DB buffer and 100 ul of aggregation-competent cells were placed in 3 ml dishes with a cover glass underneath and incubated with or without 2 mM caffeine for 1 h. The cells were uniformly stimulated by quickly pipetting 220 ul of 150 uM cAMP into the plate containing cells. The fluorescence images were taken at time-lapse intervals of 2 sec for 1 min by using an inverted microscope (IX71; Olympus) with a camera (DS-Fil; Nikon) controlled by the NIS-Elements software (Nikon) and Image J software (National Institutes of Health). The intensity of the fluorescence in the plasma membrane was measured, and the relative level of PH-CRAC was calculated by dividing the intensity before stimulation ($E_o$) with the intensity at each time point ($E_t$)

## II-4. Development

Development was performed as described previously (Jeon et al., 2009). Exponentially growing cells were harvested and washed twice with 12 mM Na/K phosphate buffer (pH 6.1) and resuspended at a density of 3.5 x $10^7$ cells/ml. 50 μl of the cells were plated and developed in non-nutrient agar plates with or without caffeine, Torin2, LY294002 and Rapamycin. The multicellular organisms were photographed and examined with a phase-contrast microscope at the indicated times in the figures.

## II-5. Statistics

Statistical analysis was performed using Student's t-test (two-tailed). All data was collected from at least three independent experiments and expressed as the means ± standard deviation (SD). P value less than 0.05 was considered as statistically significant.

# III. Results

## III-1. RapC is essential for multicellular development of *Dictyostelium*

When *Dictyostelium* cells are starved, the cells secrete cAMP, a chemoattractant. Then, they recognize cAMP and aggregate together to form multicellular aggregates. Multicellular aggregates formed in the early stages of development go through differentiation processes to form moving slugs and finally form fruiting bodies consist of a dead stalk and a mass of spores within 24 h (Loomis, 2015). In this process, normal cells form a single tip, but cells lacking RapC have been reported to form multi-tips from one multicellular aggregate (Park *et al.*, 2018).

To determine whether RapC is essential for regulating normal developmental processes, I examined the developmental phenotypes of *rapC* null cells and GFP-RapC/*rapC* null cells compared to wild-type cells (Fig. 1). Wild-type cells formed aggregates at 8 h after starvation began, elongated slugs at 12 h, and finally fruiting bodies within 24 h. *rapC* null cells failed to form slugs and formed complex aggregates at 12 h. Even at 24 h, the stalk did not rise long enough and multi-tips were formed. In RapC-overexpressing cells, the phenotypes of *rapC* null cells were restored and single tips were formed. These results suggest that RapC is essential for regulating normal multicellular development of *Dictyostelium*.

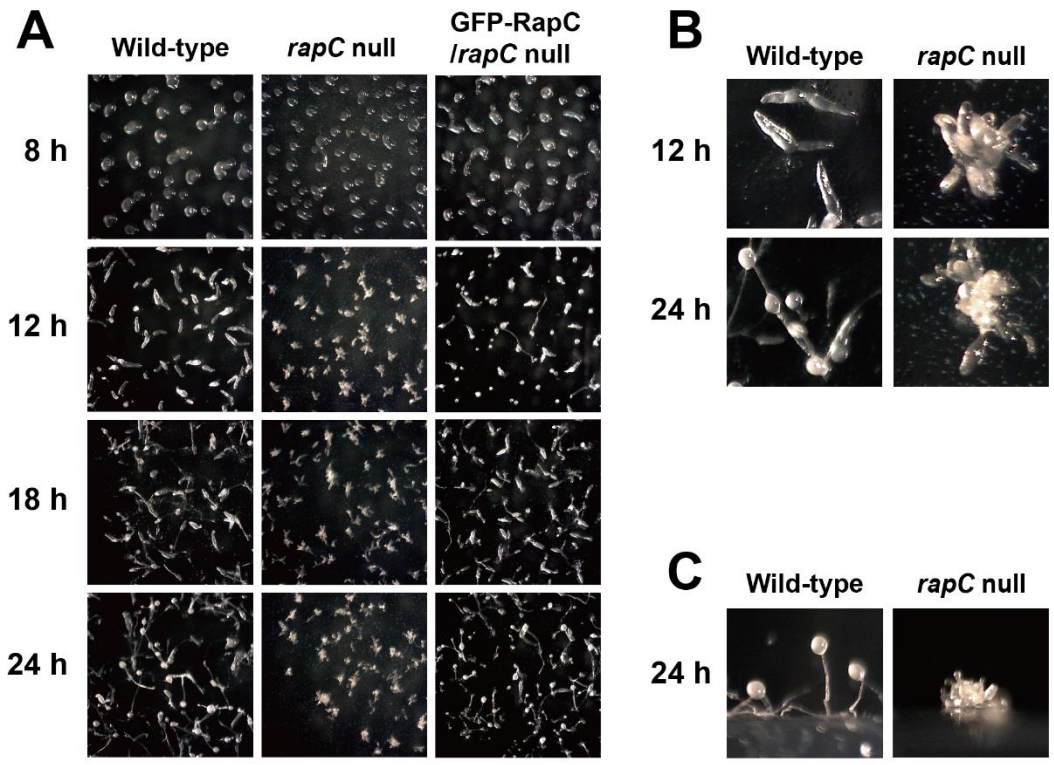


**Figure 1. Developmental phenotypes of *rapC* null cells.**

(A) Developmental phenotypes of the cells on non-nutrient agar plates. Exponentially growing cells were washed and plated on non-nutrient agar plates. Photographs were taken at the indicated times after plating and representative developmental images at the developmental stages were shown. (B) Multicellular structures of the cells at 12 h, 24 h development. (C) Side view of fruiting bodies at 24 h development

## III-2. Caffeine induces the multi-tip formation during development

Previous studies have shown that when *Dictyostelium* cells were treated caffeine, they formed multi-tips during development. In *Dictyostelium*, caffeine plays a role in inhibiting the synthesis of cAMP and it reduces cAMP levels in slugs, altering the gradient and relaying to induce tips elsewhere in the slug (Brenner and Thoms, 1984; Jaiswal *et al.*, 2012).

To determine which concentrations of caffeine causes multi-tips to occur when wild-type cells are treated, I observed the development of wild-type cells with various concentrations of caffeine (Fig.2). At 1 mM caffeine, there was no difference from untreated cells. At 2 mM caffeine, there was a delay in development time and some multi-tips were formed at 24 h. Above 3 mM, the temporal delay worsened, and development stopped after the aggregation stage. Because wild-type cells formed multi-tips at 2 mM caffeine, we also treated *rapC* null cells with 2 mM caffeine and observed the development (Fig.3). *rapC* null cells treated 2 mM caffeine showed a temporal delay occurred during development and multi-tips became more severe.

After that, while investigating whether there were additional factors affecting development of *Dictyostelium*, it was found that the central area where the tip is forming in the mound had a higher potential than the edge area (Reid et al., 2007). Therefore, I treated the wild-type cells with various concentrations of potassium, which indirectly depolarizes them, and observed the development (Fig.4). As the concentration of potassium increased, the temporal delay worsened compared to untreated cells, but finally all the cells formed single tips. These results suggest that caffeine induces multi-tip formation during development, but that electrical factors such as potassium are not involved.

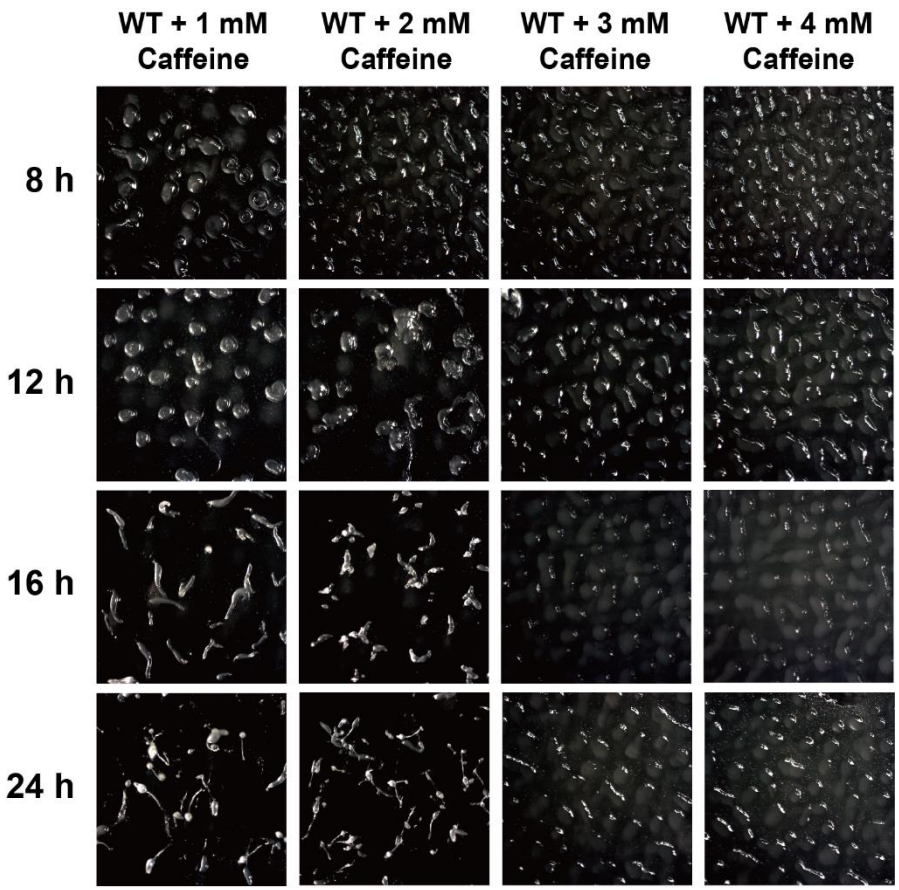


**Figure 2. Developmental phenotypes of wild-type cells at the various concentration of caffeine.**

Exponentially growing cells were washed and plated on non-nutrient agar plates with various concentrations of caffeine. Photographs were taken at the times indicated after plating. Representative developmental images at the developmental stages were presented.

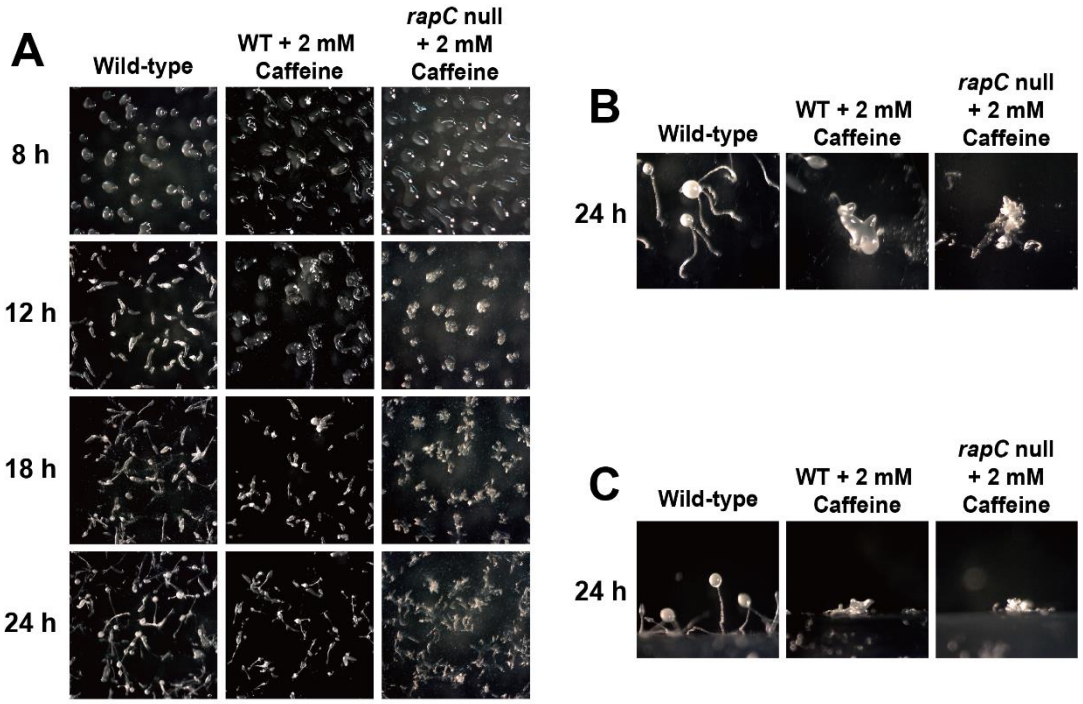


**Figure 3. Developmental phenotypes of *rapC* null cells with treatment of 2 mM caffeine.**

**(A)** Developmental phenotypes of the cells on non-nutrient agar plates. Exponentially growing cells were washed and plated on non-nutrient agar plates at the presence of 2 mM caffeine. Photographs were taken at the indicated times after plating and representative developmental images at the developmental stages were shown. (B) Multicellular structures of the cells at 24 h development. (C) Side view of fruiting bodies at 24 h development.

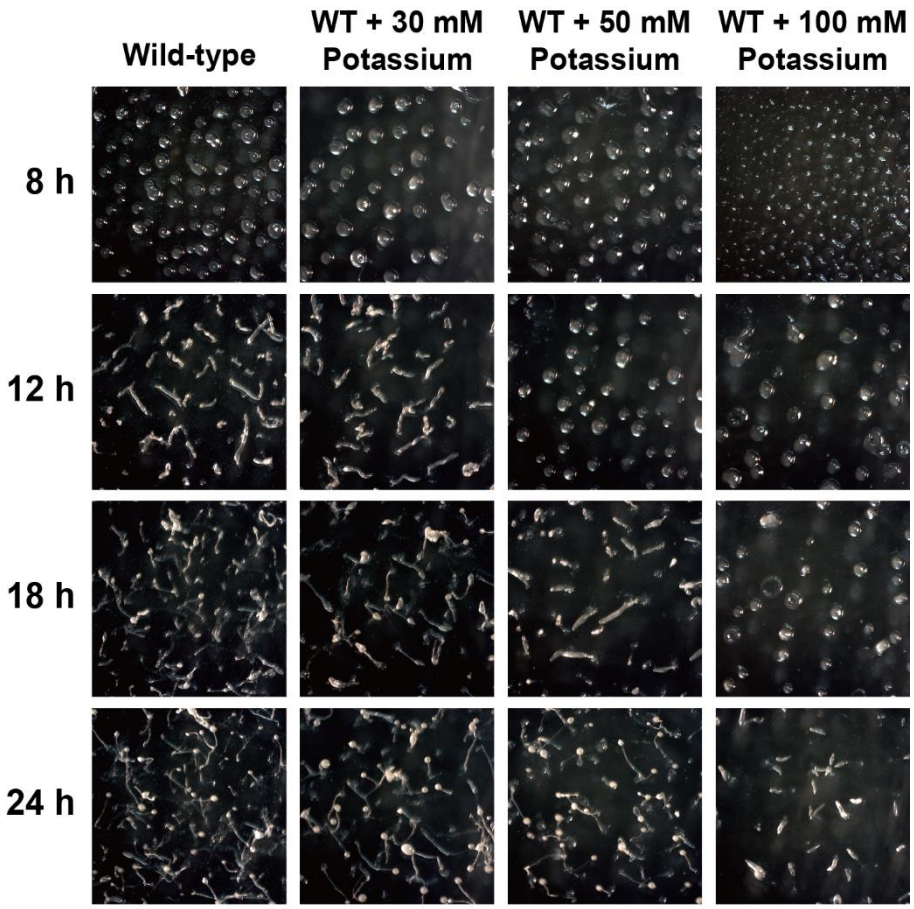


**Figure 4. Developmental phenotypes of wild-type cells at the various concentrations of potassium**

Exponentially growing cells were washed and plated on non-nutrient agar plates with various concentrations of potassium. Photographs were taken at the times indicated after plating. Representative developmental images at the developmental stages were presented.

## III-3. TOR signaling pathway is involved in multi-tips formation process

The cAMP signaling pathway in *Dictyostelium* is well known, including the key PI3K and mTORC2 pathways (Devreotes *et al.*, 2017). PI3K and mTORC2 pathways are required for ACA activation and cAMP production in response to extracellular cAMP stimulation. Caffeine inhibits cAMP synthesis mainly through the PI3K and mTORC2 pathways (Brenner and Thoms, 1984). I examined the effects of PI3K and mTORC2 on multicellular development (Fig. 5 and Fig. 6).

First, to check the PI3K signaling pathway, I examined the development of cells lacking ACA, which exist downstream of PI3K. The development of *acaA* null cells was stopped at the aggregation stage (Fig. 5A). Next, to examine the effects of PI3K on multicellular development, wild-type cells and *rapC* null cells were developed in the presence of 30 μM LY294002, an inhibitor of PI3K. Both wild-type cells and *rapC* null cells treated with LY294002 formed smaller multicellular mounds compared to untreated wild-type cells. Wild-type cells finally formed single tips in the presence of LY294002 (Fig. 5B). To identify CRAC that exists downstream of PI3K, global stimulation experiments were performed. Wild-type cells and *rapC* null cells expressing PH-crac-GFP were stimuli by cAMP, a chemoattractant, in the presence or absence of 5 mM caffeine. In the absence of caffeine treatment, there was no difference in PH-crac activity between wild-type cells and *rapC* null cells. Additionally, when both cells were treated with caffeine, their PH-crac activities were significantly reduced (Fig.5C and D). These results suggest that PI3K route is not involved in the multi-tip formation process.

To confirm whether mTORC2 pathway is involved in the multi-tip formation of RapC, wild-type cells and *rapC* null cells were developed in the presence of 1 μM Torin2, an inhibitor of mTORC2. Both wild-type cells and *rapC* null cells treated with Torin2 showed a temporal delay during development compared to untreated cells. And wild-type cells treated with Torin2 formed some multi-tips at 18 h and 24 h. This result suggests that the mTORC2 pathway is involved in the multi-tip formation process.

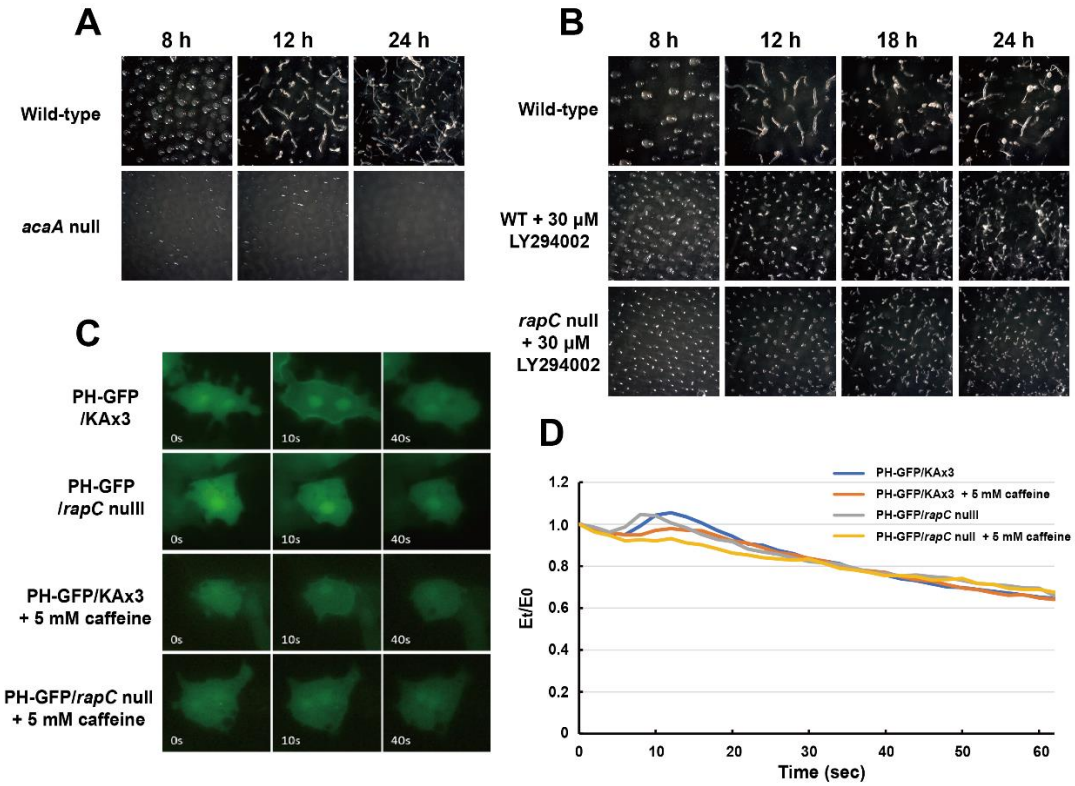


**Figure 5. Downstream of PI3K signaling pathway.**

**(A)** Developmental phenotypes of *acaA* null cells. (B) Developmental phenotypes of the cells with or without 30 μM LY294002. (C) Fluorescence of PH-CRAC proteins of aggregation-competent cells after cAMP stimulation with or without 5 mM caffeine. (D) Quantification of the cytoplasmic fluorescence intensity of aggregation-competent cells upon cAMP stimulation.

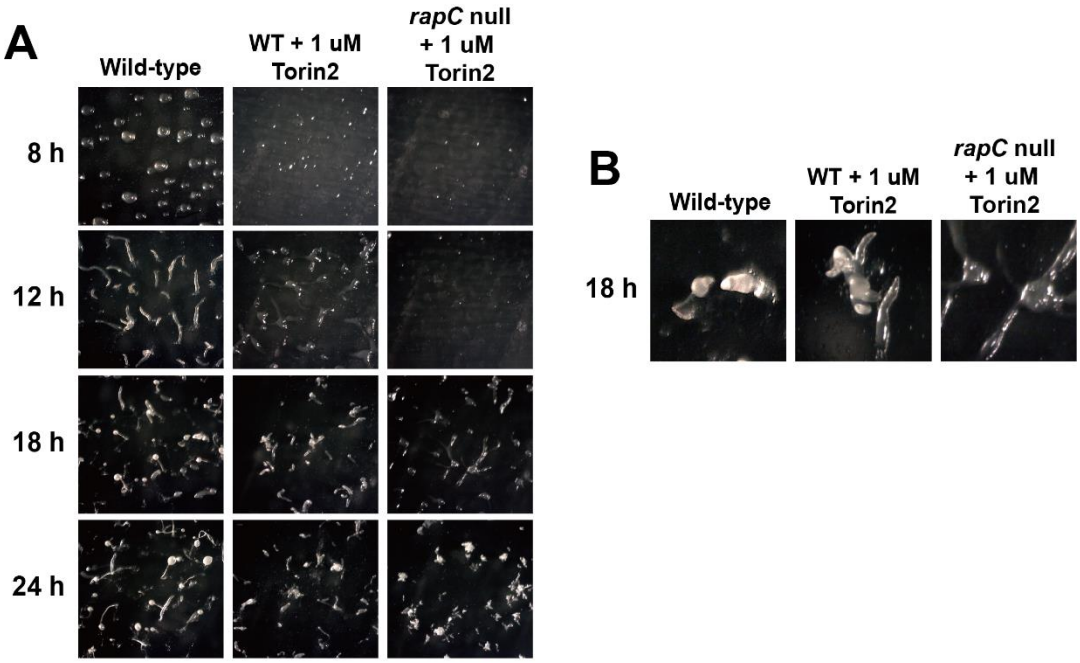


**Figure 6. Developmental phenotypes of wild-type cells and *rapC* null cells with treatment of 1 μM Torin2**.

**(A)** Developmental phenotypes of the cells in non-nutrient agar plates with or with 1 μM Torin2. Exponentially growing cells were washed and plated on non-nutrient agar plates with or without 1 μM Torin2. (B) Multicellular structures of the cells at 18 h development.

## III-4. TORC1 plays an important role in the developmental process

To determine which TOR complex affects the developmental process, I examined the multicellular development of the cells in the presence of 50 nM rapamycin, a mTORC1 inhibitor (Fig. 7). In the presence of 50 nM rapamycin, wild-type cells formed multi-tipped mounds at 12 h and multi-branched developmental structures at 14 h and 18 h. *rapC* null cells showed temporal delay in development and their multi-tips became more severe. These results suggest TORC1 has an important role in the developmental process.

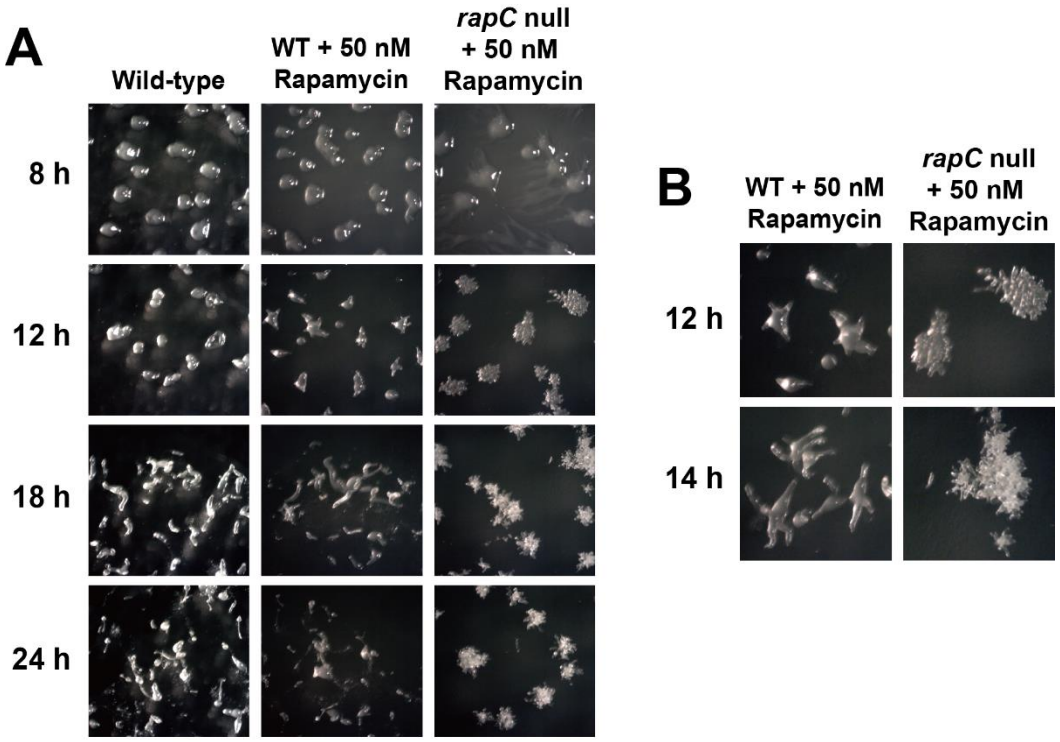


**Figure 7. Developmental phenotypes of wild-type cells and *rapC* null cells with treatment of 50 nM Rapamycin**.

**(A)** Developmental phenotypes of the cells in non-nutrient agar plates with or with 50 nM Rapamycin. Exponentially growing cells were washed and plated on non-nutrient agar plates with or without 50 nM Rapamycin. (B) Multicellular structures of the cells at 12 h and 14 h development.

# IV. Discussion

In this study, I aimed to investigate the mechanism of regulation of *Dictyostelium* development by RapC. Wild-type cells formed multi-tips in the presence of caffeine, Torin2, and rapamycin. The results suggest the possibility that the TOR signaling pathway is involved in the multi-tip formation process. To further examine this mechanism, the experiments are underway to compare the degree of phosphorylation of the PKB substrate that exists downstream of mTORC2.

In *Dictyostelium*, there are two PKB homologs, PKBA and PKBR1 (Meili et al., 2000). Upon chemoattractant stimulation, PKBA and PKBR1 are both phosphorylated within the hydrophobic motifs (HMs) through TORC2 and subsequently phosphorylated within the activation loops (ALs) by phosphoinositide-dependent kinases (PDKs) (Kamimura et al., 2008; Kamimura and Devreotes, 2010). Therefore, it is expected that there will be differences in the degree of phosphorylation of hydrophobic motifs through TORC2 between wild-type cells and *rapC* null cells. When PKBA and PKBR1 are phosphorylated, the downstream substrates are also phosphorylated (Kamimura *et al.*, 2008). Experiments examining the degree of phosphorylation of these substrates in wild-type cells and *rapC* null cells are also underway.

In this study, Wild-type cells formed of multi-tips when treated with 50 nM rapamycin (Fig.7). TORC1 is well known as major nutrient sensors that control the responses to changes in nutrient and energy levels (Saxton and Sabatini, 2017). During development, mTORC1 is activated complementary to AMP-activated protein kinase (AMPK). In cell growth state, mTORC1 is activated and AMPK activity is suppressed. However, when starvation begins, the activity of mTORC1 rapidly decreased and AMPK becomes activated. Therefore, AMPK activity is high in the aggregation stage (Rattan et al., 2005; Rosel et al., 2012). This suggests that inhibition of mTORC1 may induce AMPK activity, resulting in hyper aggregation at the aggregation stage. TORC1 is known to be involved in autophagy in *Dictyostelium* (Calvo-

Garrido et al., 2010). It is also known that deletion of some of the autophagy factors also leads to multi-tip formation during development (Mesquita et al., 2017). These suggest that the possibility that RapC is involved in autophagy through mTORC1 regulation.

# PART II. Functional Changes of Ras Proteins by C-terminus of RapC

## I. Introduction

Ras proteins cycle between the GTP-bound active state and the GDP-bound inactive state. Through this cycle, they act as molecular switches involved in several cellular processes (Raaijmakers and Bos, 2009). The activity of Ras proteins is regulated by guanine nucleotide exchange factors (GEFs) and GTPase-activating proteins (GAPs). GEFs are exchange factors that catalyze GTP binding. GAPs return activated Ras to inactive by enhance GFP hydrolysis (Mun et al., 2014). The regulation of Ras proteins is important because when their activity is impaired, it affects multiple downstream signaling pathways and causes mutations (Downward, 2003).

*Dictyostelium*, a social amoeba, has Ras subfamily proteins consisting of 11 Ras, 3 Rap, and 1 Rheb. Among them, the Rap proteins composed of RapA, RapB, and RapC. RapA is known to be a key regulator of cell adhesion through F-actin assembly and myosin degradation in response to external stimuli (Kortholt and van Haastert, 2008; Hilbi and Kortholt, 2019). The functions of RapB are still unknown, but it is predicted to have a similar function to RapA, with which it has the highest genetic homology. RapC is known to have opposite functions to RapA in cell adhesion and cell migration. RapA enhances cell adhesion and reduces cell migration, whereas RapC plays a negative role in cell adhesion and enhances cell migration (Jeon et al., 2021).

RapC consists of 278 amino acids and has a longer tail sequence in the C-terminus region compared to RapA, which consists of 186 amino acids. Previous studies have shown that when

the C-terminus region of RapC was fused to the end of RapA, the functions of RapA in cell migration and cell adhesion are reversed and in acts like RapC. When recombinant RapA-CT was expressed in *rapC* null cells, the phenotypes of *rapC* null cells were completely restored, including cell adhesion, motility, and development (Kim et al., 2021).

In this study, to determine whether the C-terminus of RapC can reverse the functions of other Ras proteins, I fused the C-terminus of RapC to the end of RasG, which has the most similar function to RapA among Ras proteins. Recombinant RasG-CT was expressed in *rapC* null and *rasG* null cells, and the phenotypes were compared those of wild-type cells.

# II. Materials and Methods

## II-1. Strains and plasmids

*Dictyostelium* wild-type KAx3 cells were cultured axenically in HL5 medium at 22 ℃. For expression of GFP-RasG-CT, the full coding sequence of RasG-CT was generated by Gibson assembly. Each primer has an *EcoR* I site, the RasG-specific sequences, and sequences that overlap with RapC, or an *Xho* I site, the RapC-specific sequences, and sequences that overlap with RasG. Full-length RasG-CT was digested with *EcoR* 1/*Xho* I restriction enzymes and cloned into the *EcoR* I -*Xho* I site of the expression vector pEXP-4( +) containing a GFP fragment . The full coding sequence of DydA was confirmed by sequencing and transformed into *rapC* null cells and *rasG* null cells. The cells were maintained in 10 mg/ml of G418.

## II-2. Cell-substrate adhesion

Fully grown cells on plates were washed with 12 mM Na/K phosphate buffer (pH 6.1) and resuspended at the density of 3.5 x $10^7$ cells/ml. Cells (3.5 x $10^6$ in 100 ul) were plated and attached on 6-well culture dishes. After 30 min incubated, cells were photographed and counted for calculating the total cell number. The plates were constantly shaken at 150 rpm for 30 min to detach the cells from the 6-well plates. After shaking the plates, the medium containing detached cells was removed and the attached cells were photographed and counted. Cell adhesion was shown as a percentage of attached cells compared with total cells.

**Table 1. PCR primers used for RasG-CT**

| Name | Forward primer | Reverse primer |
|---|---|---|
| RasG | CCCGAATTCATGACAGAATAC AAATTAGTT | AAAATGATTGTAAAAGAGTA CAAGCTTTTAATG |
| RapC | TACTCTTTTACAATCATTTTT AAATGGATC | CCCCTCGAGCATGATTAAAC ATTTTCCTTTT |

## II-3. Development

Development was performed as described previously (Jeon *et al.*, 2009). Exponentially growing cells were harvested and washed twice with 12 mM Na/K phosphate buffer (pH 6.1) and resuspended at a density of 3.5 x $10^7$ cells/ml. 50 μl of the cells were plated and developed in non-nutrient agar plates. The multicellular organisms were examined and captured with a phase-contrast microscope.

## II-4. Chemotaxis

Exponentially growing cells were washed twice with 12 mM Na/K phosphate buffer (pH 6.1) and resuspended at a density of 5 x $10^6$ cells/ml. Aggregation-competent cells were prepared by pulsing with 30 nM cAMP every 5min for 6 h in 12 mM Na/K phosphate buffer (pH 6.1) with a constant shaking (150 rpm). Cell migration was analyzed using a Under Agarose Assay chamber. The images of chemotaxing cells were taken at time-lapse intervals of 1 min for 1 h using an inverted microscope (IX71; Olympus) with a camera (DS-Fil; Nikon). The data were analyzed using the NIS-elements software (Nikon) and Image J software (National Institutes of Health, NIH). Trajectory speed was used to quantify motility of the cells. The trajectory speed is the total distance moved of a cell every 1 min in a time-lapse recording. Directionality is measure of how straight the cells move. Cells moving in a straight line have a directionality of 1. It was calculated as the distance moved over the linear distance between the start and the finish.

## II-5. Electrotaxis

Electrotaxis assay using semi-vegetative cells was performed as described previously (Jeon et al., 2019). Fully grown cells on 24-well plates were washed with development buffer (DB; 5 mM $Na_2HPO_4$, 5 mM $KH_2PO_4$, 2 mM $MgCl_2$ and 1 mM $CaCl_2$) and incubated 3 h in 1 ml of DB buffer to prepare semi-vegetative cells. The developed cells were resuspended and seeded in an electrotactic chamber for 20 min and the attached cells were washed off using 50 μl of DB buffer. A roof of cover glass was placed on the cells within a through and sealed with silicone grease. Each chamber was filled with sufficient DB. EF was applied at the indicated field strength through agar salt bridges. Cell migration was recorded at intervals of 1 min for 1 h using an inverted microscope (IX71; Olympus) with a camera (DS-Fil; Nikon) controlled by the NIS-Elements software (Nikon).

Time lapse recording of cells migration were analyzed using ImageJ software (National Institutes of Health, NIH). Directedness quantifies how directionally cells migrate in response to an EF. The directedness of the movement of the cells was measured as cosine θ, where θ is the angle between the direction of the field and a straight line connecting the start and end positions of the cell. Trajectory speed was assessed by dividing the total distance travelled by the cell by time. All data were obtained and analyzed from at least three independent experiments. The kinetics of directedness and trajectory speed were calculated by measuring the directedness and trajectory speed of cell migration every 1 min in a time-lapse recording and sequentially plotting the readings against time.

## II-6. Random migration

Random migration assay performed as described previously (Litschko et al., 2018). Vegetative fully grown in 100 mm cell culture plate were resuspended. 50 μl of the cells suspension were added to 30mm culture plate containing 3mL of Na/K phosphate buffer (pH 6.1) and allowed to adhere to the plate for 30min. Cell migration was recorded at intervals of 1 min for 30 min using an inverted microscope (IX71; Olympus) with a camera (DS-Fil; Nikon) controlled by the NIS-Elements software (Nikon).

## II-7. Statistics

Statistical analysis was performed using Student's t-test (two-tailed). All data was collected from at least three independent experiments and expressed as the means ± standard deviation (SD). P value less than 0.05 was considered as statistically significant.

# III. Results

## III-1. Complementation of rapC null cells by RasG-CT

To determine whether RasG-CT complement the phenotypes of *rapC* null cells, RasG-CT was expressed in *rapC* null cells. *rapC* null cells are known to have spread cell morphology and increased adhesion than wild-type cells. *rapC* null cells formed multi-tips during development and showed reduced migration speed during chemotaxis (Park *et al.*, 2018).

In cell size and adhesion, wild-type cells were about 120 μm$^2$ in size and their cell-substrate adhesion was about 70%. *rapC* null cells were over 200 μm$^2$ in size, about twice as large as the wild-type cells and their cell-substrate adhesion was about 90%. GFP-RasG/*rapC* null and GFP-RasG-CT/*rapC* null cells were about 200 μm$^2$ in cell size and their adhesion was about 90%, which was similar to *rapC* null cells (Fig.1).

In development, wild-type cells formed multicellular aggregates at 8 h, elongated slugs at 12 h, and finally fruiting bodies at 24 h. On the other hand, *rapC* null, GFP-RasG/*rapC* null, and GFP-RasG-CT/*rapC* null cells formed aggregates rather than elongated slugs at 12 h and formed multi-tips at 24 h (Fig.2).

In chemotaxis, wild-type cells showed a migration speed of approximately 9 μm/min and their directionality close to 1. *rapC* null, GFP-RasG/*rapC* null, and GFP-RasG-CT/*rapC* null cells showed migration speed of approximately 4-5 μm/min and their directionality was similar to wild-type cells. (Fig.3). These results suggest that the expression of RasG-CT is unable to complement the phenotypes of *rapC* null cells.

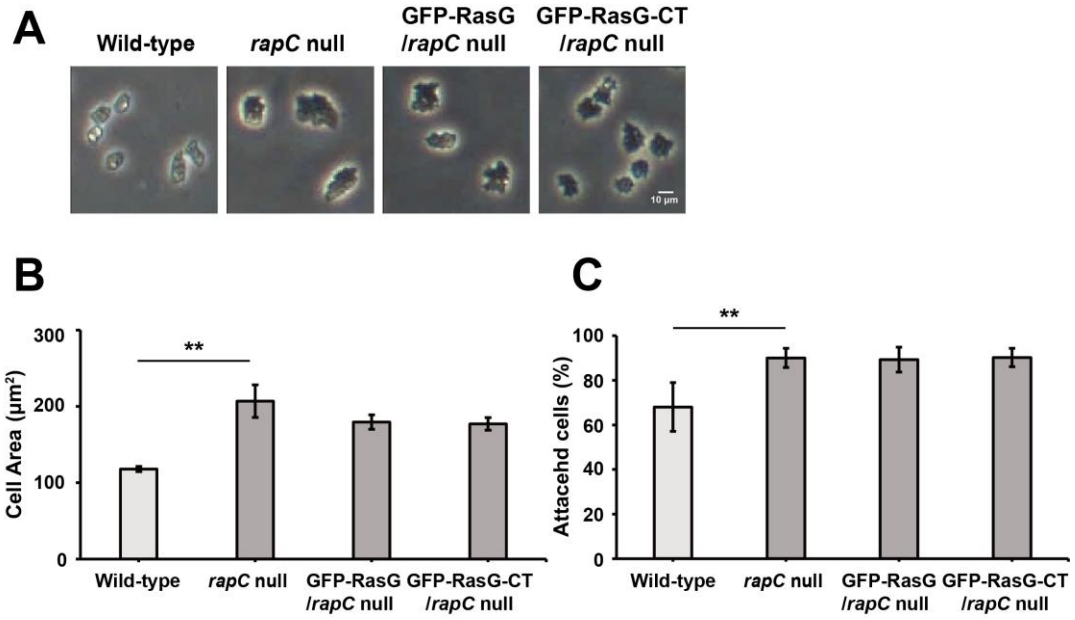


**Fig. 1. Cell morphology and adhesion of *rapC* null cells.**

(A) Morphology of the vegetative cells. Wild-type KAx3, *rapC* null, GFP-RasG/*rapC* null, GFP-RasG-CT/*rapC* null were photographed. (B) Measurement of cell areas of cells using NIS-element software. Error bar represent ±SD of three independent experiments. (C) Cell-substrate adhesion. Adhesion of the cells to the substrate was expressed as a percentage of attached cells to total cells. Error bar represent ±SD of three independent experiments.

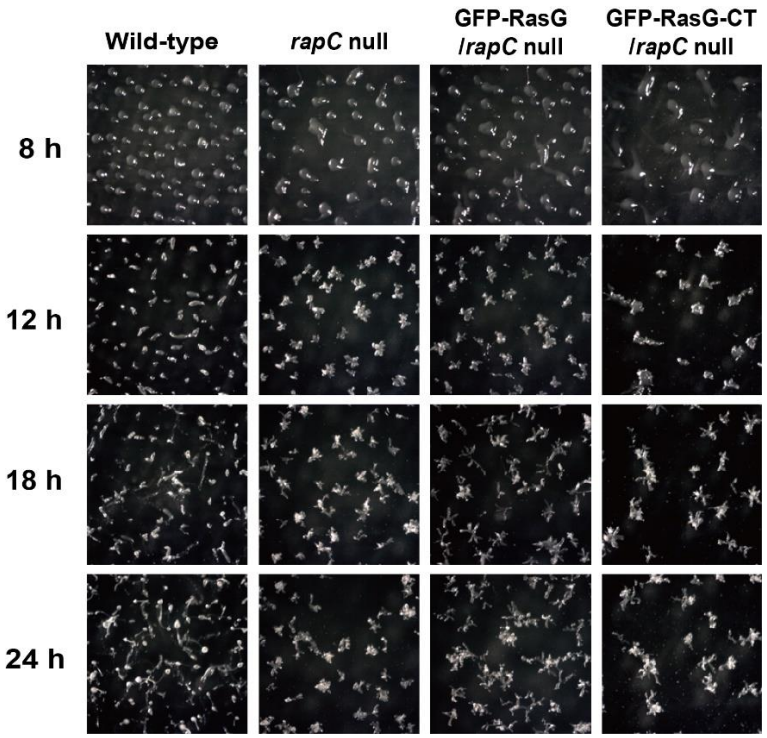


**Fig.2. Multicellular development of *rapC* null cells.**

Exponentially growing cells were washed and plated on non-nutrient agar plates. Photographs were taken at the times indicated after plating. Representative developmental images at the developmental stages were presented.

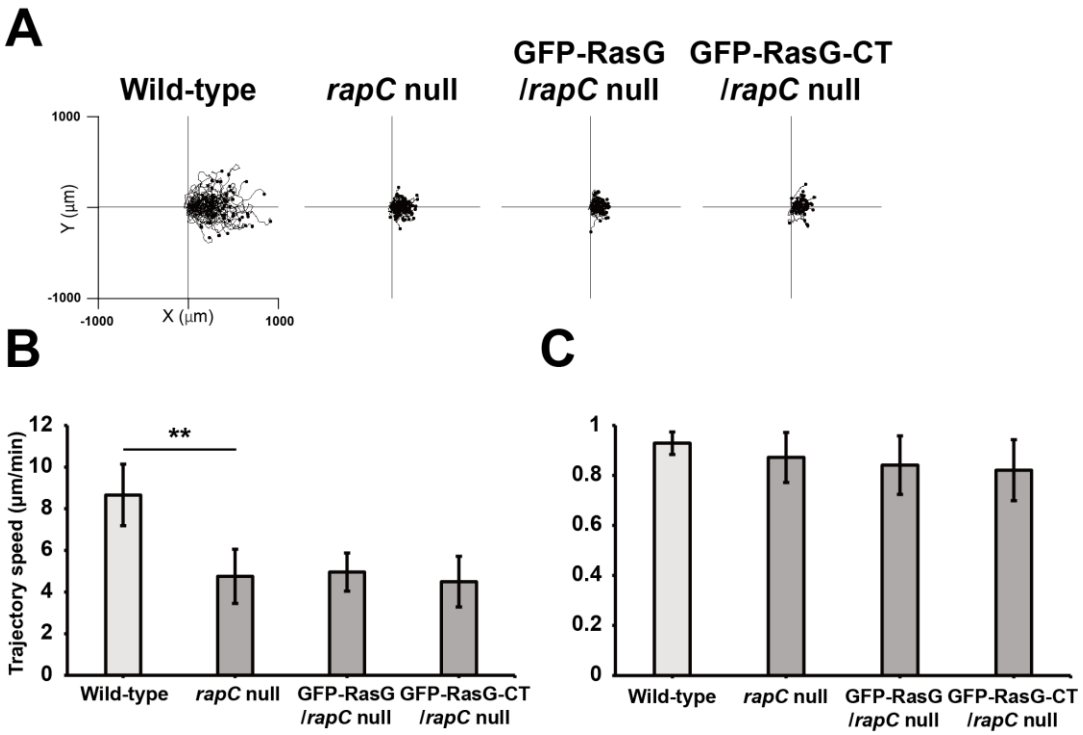


**Figure.3. Cell motility of *rapC* null cells in chemotaxis.**

Aggregation-competent cells were prepared and the placed in Under-agarose chemotaxis chamber. Movements of the cells were recorded at intervals of 1 min for 1 h. (A) Trajectories of the cells moving towards a gradient of cAMP chemoattractants. Plots show migration path of the cells with the start position of each cell centered at point 0.0. Each line represents the track of a single cell chemotaxing toward 150 μM cAMP. (B) Quantification of cell motility. Trajectories of cells during chemotaxis were traced and analyzed by using chemotaxis and migration tool in ImageJ software. Trajectory speed indicates the speed of the cell movements along the total path. Directionality is a measure of how straight the cells move. Cells migrating in a straight line have a directionality of 1.

## III-2. Complementation of *rasG* null cells by RasG-CT

To determine whether the RasG-CT complement the phenotypes of *rasG* null cells, RasG-CT was expressed in *rasG* null cells. Therefore, we observed the phenotypes of *rasG* null, GFP-RasG/*rasG* null, and GFP-RasG-CT/*rasG* null cells in several experiments including electrotaxis to determine whether expression of RasG-CT can complement the phenotypes of *rasG* null cells.

First, we compared the cell sizes of wild-type cells and *rasG* null, GFP-RasG/*rasG* null, GFP-RasG-CT/*rasG* null cells. The size of wild-type cells was about 120 μm$^2$. *rasG* null cells showed spread morphology compared to wild-type cells. GFP-RasG/*rasG* null, GFP-RasG-CT/*rasG* null cells were similar in size to wild-type cells (Fig.4). In development, wild-type cells formed multicellular aggregates at 8 h, elongated slugs at 12 h, and finally fruiting bodies at 24 h. *rasG* null cells formed smaller multicellular aggregates compared to wild-type cells at 12 h and formed fruiting bodies at 24 h. GFP-RasG/*rasG* null and GFP-RasG-CT/*rasG* null cells formed multi-tips at 24 h (Fig.5).

After that, to compare the random migration of cells, we conducted a random motility experiment with a vegetative state to compare cell migration in the absence of stimulation. Wild-type cells showed a migration speed of about 3-4 μm/min, whereas *rasG* null cells showed a migration speed of about 8 μm/min, which is more than twice that of wild-type. The migration speed of GFP-RasG/*rasG* null and GF-RasG-CT/*rasG* null cells was similar to wild-type.

Additionally, RasG is known to be essential for EF-induced directionality (Jeon *et al.*, 2019). To compare cell movement by electrical factors, electrotaxis experiments were conducted in a semi-vegetative state in which each cell was allowed to develop for 3 h. Before applying electricity, wild-type cells showed a migration speed of 1-2 μm/min and almost no directionality. During EF when electrical stimulation was given, the speed was approximately 4, and the directionality was close to 1. After the electrical stimulation disappeared, the speed decreased again to about 2 μm/min, and the directionality also decreased. rasG null cells showed a speed

of about 7 μm/min in Before, and a speed of about 10 μm/min in EF, which is more than twice that of wild-type cells. And after the electrical stimulation ended, the speed was around 7 μm/min. The directionality of *rasG* null cells was close to 0 in all before, EF, and after. Similar to wild-type cells, GFP-RasG/*rasG* null and GFP-RasG-CT/*rasG* null cells had slow and undirected movement before and after electrical stimulation, but when electrical stimulation was given, their movement speed increased, and directionality increased that was close to 1.

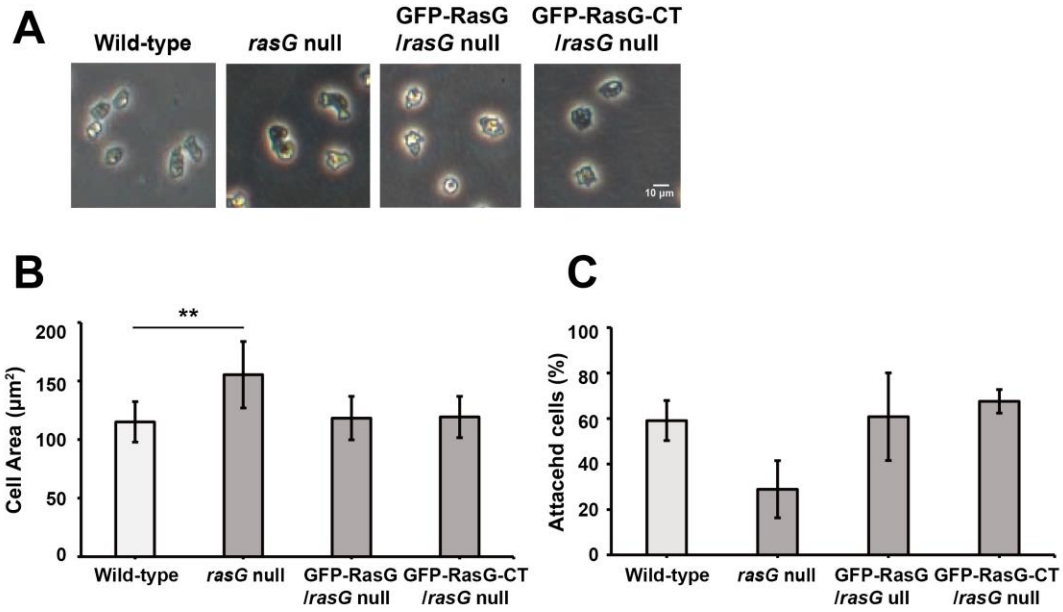


**Fig. 4. Cell morphology and adhesion of *rasG* null cells.**

(A) Morphology of the vegetative cells. Wild-type KAx3, *rasG* null, GFP-RasG/*rasG* null, GFP-RasG-CT/*rasG* null were photographed. (B) Measurement of cell areas of cells using NIS-element software. Error bar represent ±SD of three independent experiments. (C) Cell-substrate adhesion. Adhesion of the cells to the substrate was expressed as a percentage of attached cells to total cells. Error bar represent ±SD of three independent experiments.

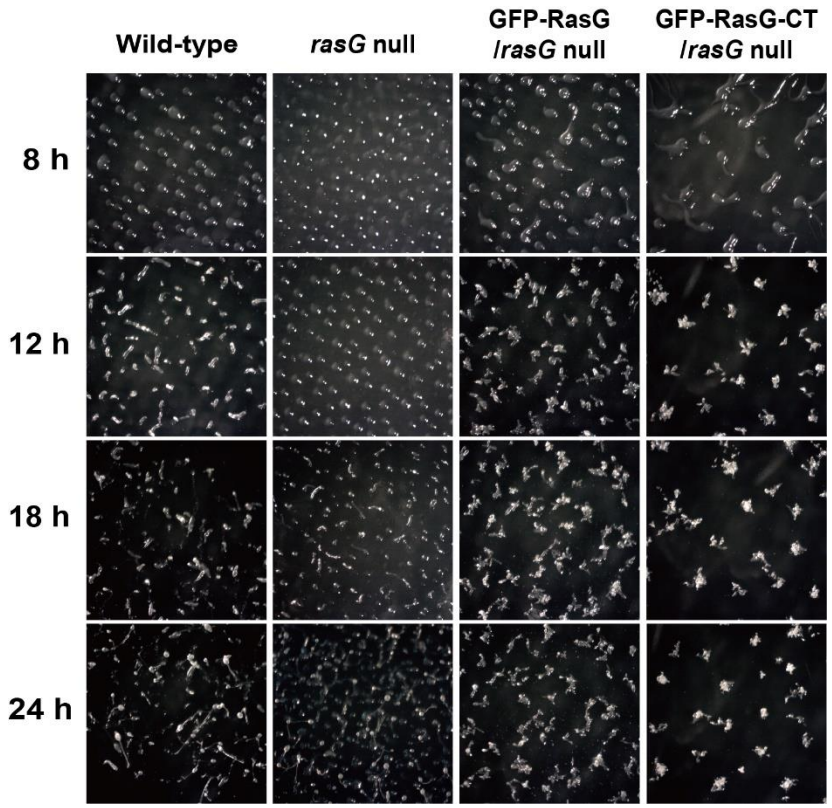


**Fig.5. Multicellular development of *rasG* null cells.**

Exponentially growing cells were washed and plated on non-nutrient agar plates. Photographs were taken at the times indicated after plating. Representative developmental images at the developmental stages were presented.

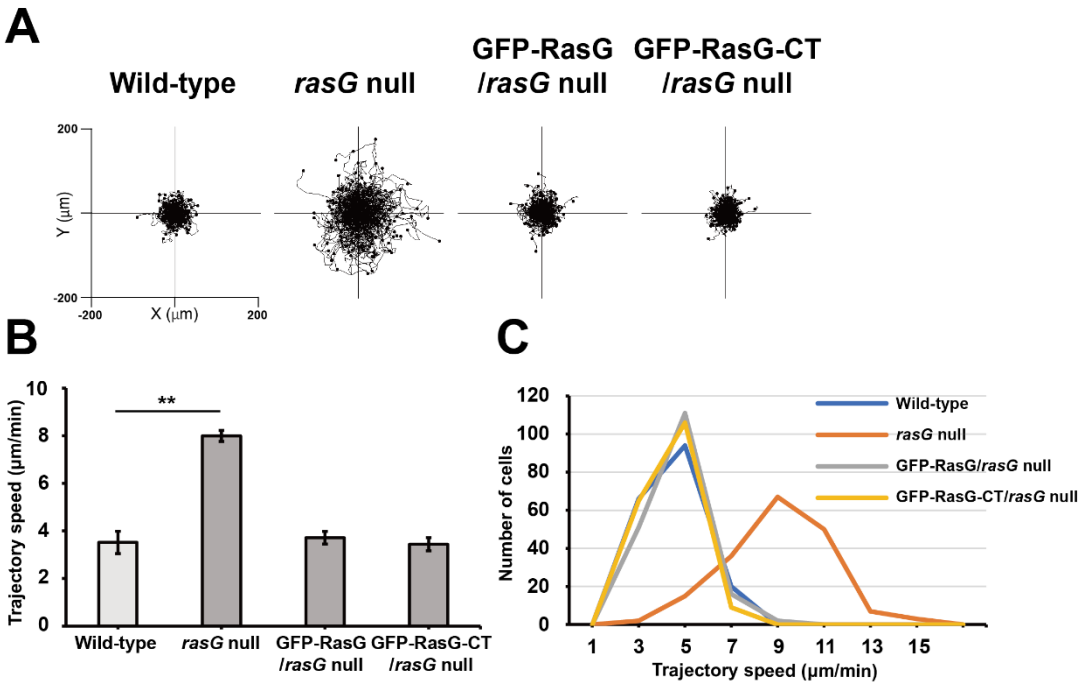


**Fig.6. Random motility of *rasG* null cells.**

(A) Trajectories of *rasG* null cells in random migration. Plots show migration paths of the cells with the start position of each cell centered at point 0,0. (B) Quantification of migration speed of *rasG* null cells. Data are means ± S.E.M. from three independent experiments and statistical analysis was performed using the Student's t-test, *P<0.05, **P<0.01.

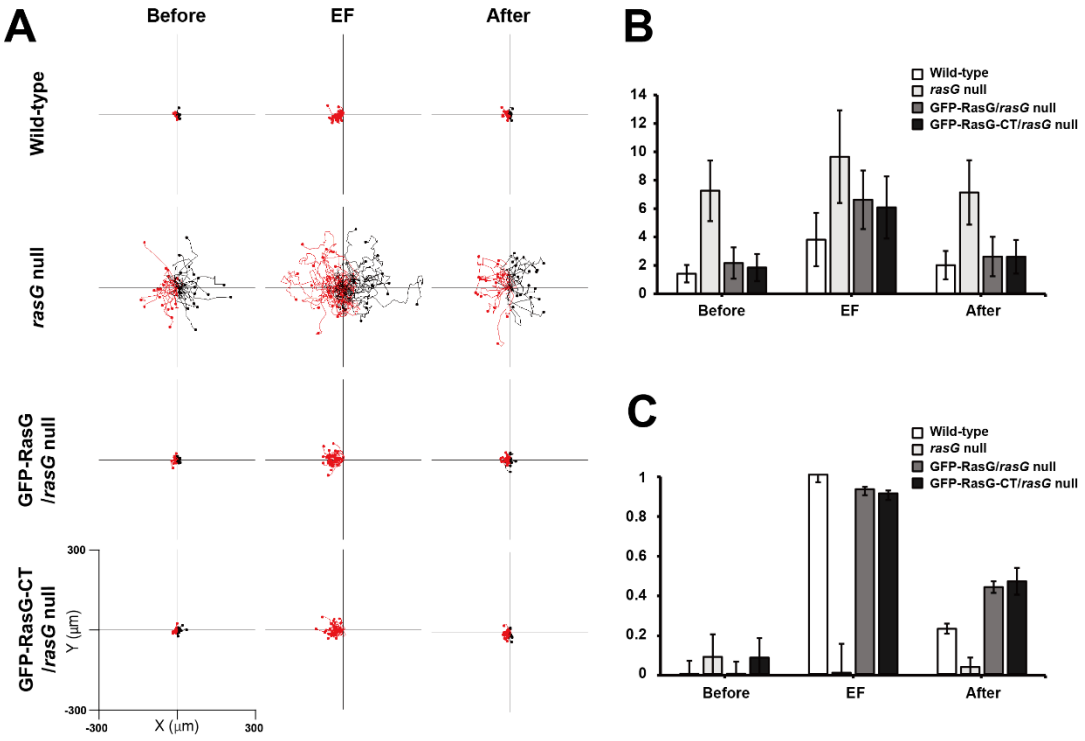


**Figure.7. Electrotactic responses of *rasG* null cells in the semi-vegetative state.**

(A) Trajectories of wild-type KAx3, *rasG* null, GFP-RasG/*rasG* null, and GFP-RasG-CT/*rasG* null cells (Before 1~10 min, EF 31~40min, and After 41~50 min). (B) Quantitative analysis of the trajectory speed of *rasG* null cells. (C) Quantitative analysis of the directional migration of *rasG* null cells. Data are means ± S.E.M. from three independent experiments in an EF of 15 V/cm.

# IV. Discussion

In this study, to determine whether the C-terminus region of RapC can reverse the functions of RasG, we produced recombinant RasG-CT by fusing the C-terminus of RapC to the end of RasG. RasG-CT was expressed respectively in *rapC* null and *rasG* null cells. As a result, the expression of RasG-CT restored the phenotypes of *rasG* null cells, not *rapC* null cells. This suggest that the C-terminus of RapC is able to reverse the functions of the Rap proteins, but not other Ras proteins.

To investigate why the functional reversal of the C-terminus of RapC applies only to RapA, additional protein analysis was performed. There is a difference in the length of the C-terminus sequence of RapC used in the experiment. The C-terminus region fused to RapA in a previous study was 92 amino acids and the C-terminus fused to RasG in this study was 107 amino acids (Jeon *et al.*, 2021). To determine whether there are differences in function depending on the length of the C-terminus, it is necessary to examine the expression of only the C-terminus of the length fused to RasG.

RasG had more lysines than RapA in the variable region. In previous studies, it was found that positive amino acids present in the variable region interact with the plasma membrane and play an important role in signal transmission through the nanoclusters (Zhou and Hancock, 2015). For Ras proteins to be active, they must form transient nanoclusters on the plasma membrane. Nanoclusters are the sites for effector recruitment and activation, so essential for Ras signaling (Tian et al., 2007). In mammalian, the K-Ras isoform has multiple lysines in the hypervariable region (Prior and Hancock, 2001). When K-Ras is activated by GTP binding, it interacts with plasma membrane through hypervariable region interaction. Since the inside of the plasma membrane is negatively charged, positive amino acids present in the variable region are involved in the interaction (Zhou and Hancock, 2015). This suggests that there are differences in Ras

activation due to the positive amino acids present in the variable region between Ras and Rap proteins.

# References

Chisholm, R.L., and Firtel, R.A. (2004). Insights into morphogenesis from a simple developmental system. Nat Rev Mol Cell Biol *5*, 531-541. 10.1038/nrm1427.

Williams, J.G. (2006). Transcriptional regulation of Dictyostelium pattern formation. EMBO Rep *7*, 694-698. 10.1038/sj.embor.7400714.

Loomis, W.F. (2015). Genetic control of morphogenesis in Dictyostelium. Dev Biol *402*, 146-161. 10.1016/j.ydbio.2015.03.016.

Kortholt, A., and van Haastert, P.J. (2008). Highlighting the role of Ras and Rap during Dictyostelium chemotaxis. Cell Signal *20*, 1415-1422. 10.1016/j.cellsig.2008.02.006.

Raaijmakers, J.H., and Bos, J.L. (2009). Specificity in Ras and Rap signaling. J Biol Chem *284*, 10995-10999. 10.1074/jbc.R800061200.

Park, B., Kim, H., and Jeon, T.J. (2018). Loss of RapC causes defects in cytokinesis, cell migration, and multicellular development of Dictyostelium. Biochem Biophys Res Commun *499*, 783-789. 10.1016/j.bbrc.2018.03.223.

Brenner, M., and Thoms, S.D. (1984). Caffeine blocks activation of cyclic AMP synthesis in Dictyostelium discoideum. Dev Biol *101*, 136-146. 10.1016/0012-1606(84)90124-6.

Jaiswal, P., Singh, S.P., Aiyar, P., Akkali, R., and Baskar, R. (2012). Regulation of multiple tip formation by caffeine in cellular slime molds. BMC Dev Biol *12*, 26. 10.1186/1471-213X-12-26.

Devreotes, P.N., Bhattacharya, S., Edwards, M., Iglesias, P.A., Lampert, T., and Miao, Y. (2017). Excitable Signal Transduction Networks in Directed Cell Migration. Annu Rev Cell Dev Biol *33*, 103-125. 10.1146/annurev-cellbio-100616-060739.

Tariqul Islam, A.F.M., Scavello, M., Lotfi, P., Daniel, D., Haldeman, P., and Charest, P.G. (2019). Caffeine inhibits PI3K and mTORC2 in Dictyostelium and differentially affects

multiple other cAMP chemoattractant signaling effectors. Mol Cell Biochem *457*, 157-168. 10.1007/s11010-019-03520-z.

Jeon, T.J., Lee, D.J., Merlot, S., Weeks, G., and Firtel, R.A. (2007). Rap1 controls cell adhesion and cell motility through the regulation of myosin II. J Cell Biol *176*, 1021-1033. 10.1083/jcb.200607072.

Jeon, T.J., Lee, S., Weeks, G., and Firtel, R.A. (2009). Regulation of Dictyostelium morphogenesis by RapGAP3. Dev Biol *328*, 210-220. 10.1016/j.ydbio.2009.01.016.

Reid, B., Nuccitelli, R., and Zhao, M. (2007). Non-invasive measurement of bioelectric currents with a vibrating probe. Nat Protoc *2*, 661-669. 10.1038/nprot.2007.91.

Meili, R., Ellsworth, C., and Firtel, R.A. (2000). A novel Akt/PKB-related kinase is essential for morphogenesis in Dictyostelium. Curr Biol *10*, 708-717. 10.1016/s0960-9822(00)00536-4.

Kamimura, Y., Xiong, Y., Iglesias, P.A., Hoeller, O., Bolourani, P., and Devreotes, P.N. (2008). PIP3-independent activation of TorC2 and PKB at the cell's leading edge mediates chemotaxis. Curr Biol *18*, 1034-1043. 10.1016/j.cub.2008.06.068.

Kamimura, Y., and Devreotes, P.N. (2010). Phosphoinositide-dependent protein kinase (PDK) activity regulates phosphatidylinositol 3,4,5-trisphosphate-dependent and -independent protein kinase B activation and chemotaxis. J Biol Chem *285*, 7938-7946. 10.1074/jbc.M109.089235.

Saxton, R.A., and Sabatini, D.M. (2017). mTOR Signaling in Growth, Metabolism, and Disease. Cell *169*, 361-371. 10.1016/j.cell.2017.03.035.

Rattan, R., Giri, S., Singh, A.K., and Singh, I. (2005). 5-Aminoimidazole-4-carboxamide-1-beta-D-ribofuranoside inhibits cancer cell proliferation in vitro and in vivo via AMP-activated protein kinase. J Biol Chem *280*, 39582-39593. 10.1074/jbc.M507443200.

Rosel, D., Khurana, T., Majithia, A., Huang, X., Bhandari, R., and Kimmel, A.R. (2012). TOR complex 2 (TORC2) in Dictyostelium suppresses phagocytic nutrient capture

independently of TORC1-mediated nutrient sensing. J Cell Sci *125*, 37-48. 10.1242/jcs.077040.

Calvo-Garrido, J., Carilla-Latorre, S., Kubohara, Y., Santos-Rodrigo, N., Mesquita, A., Soldati, T., Golstein, P., and Escalante, R. (2010). Autophagy in Dictyostelium: genes and pathways, cell death and infection. Autophagy *6*, 686-701. 10.4161/auto.6.6.12513.

Mesquita, A., Cardenal-Munoz, E., Dominguez, E., Munoz-Braceras, S., Nunez-Corcuera, B., Phillips, B.A., Tabara, L.C., Xiong, Q., Coria, R., Eichinger, L., et al. (2017). Autophagy in Dictyostelium: Mechanisms, regulation and disease in a simple biomedical model. Autophagy *13*, 24-40. 10.1080/15548627.2016.1226737.

Mun, H., Lee, M.R., and Jeon, T.J. (2014). RapGAP9 regulation of the morphogenesis and development in Dictyostelium. Biochem Biophys Res Commun *446*, 428-433. 10.1016/j.bbrc.2014.01.196.

Downward, J. (2003). Targeting RAS signalling pathways in cancer therapy. Nat Rev Cancer *3*, 11-22. 10.1038/nrc969.

Hilbi, H., and Kortholt, A. (2019). Role of the small GTPase Rap1 in signal transduction, cell dynamics and bacterial infection. Small GTPases *10*, 336-342. 10.1080/21541248.2017.1331721.

Jeon, J., Kim, D., and Jeon, T.J. (2021). Opposite functions of RapA and RapC in cell adhesion and migration in Dictyostelium. Anim Cells Syst (Seoul) *25*, 203-210. 10.1080/19768354.2021.1947372.

Kim, D., Kim, W., and Jeon, T.J. (2021). Reversible function of RapA with the C-terminus of RapC in Dictyostelium. J Microbiol *59*, 848-853. 10.1007/s12275-021-1400-5.

Jeon, T.J., Gao, R., Kim, H., Lee, A., Jeon, P., Devreotes, P.N., and Zhao, M. (2019). Cell migration directionality and speed are independently regulated by RasG and Gbeta in Dictyostelium cells in electrotaxis. Biol Open *8*. 10.1242/bio.042457.

Litschko, C., Damiano-Guercio, J., Bruhmann, S., and Faix, J. (2018). Analysis of Random Migration of Dictyostelium Amoeba in Confined and Unconfined Environments. Methods Mol Biol *1749*, 341-350. 10.1007/978-1-4939-7701-7_24.

Zhou, Y., and Hancock, J.F. (2015). Ras nanoclusters: Versatile lipid-based signaling platforms. Biochim Biophys Acta *1853*, 841-849. 10.1016/j.bbamcr.2014.09.008.

Tian, T., Harding, A., Inder, K., Plowman, S., Parton, R.G., and Hancock, J.F. (2007). Plasma membrane nanoswitches generate high-fidelity Ras signal transduction. Nat Cell Biol *9*, 905-914. 10.1038/ncb1615.

Prior, I.A., and Hancock, J.F. (2001). Compartmentalization of Ras proteins. J Cell Sci *114*, 1603-1608. 10.1242/jcs.114.9.1603.